THE PLANCK MISSION: RECENT RESULTS, COSMOLOGICAL AND FUNDAMENTAL PHYSICS PERSPECTIVES

NAZZARENO MANDOLESI

ASI, Viale Liegi 26, Roma, Italy[*]
Dipartimento di Fisica e Scienze della Terra, Università degli Studi di Ferrara, Via Giuseppe Saragat 1, I-44122 Ferrara, Italy
INAF–IASF Bologna, Via Piero Gobetti 101, I-40129 Bologna, Italy
mandolesi@iasfbo.inaf.it

CARLO BURIGANA

INAF–IASF Bologna, Via Piero Gobetti 101, I-40129 Bologna, Italy
Dipartimento di Fisica e Scienze della Terra, Università degli Studi di Ferrara, Via Giuseppe Saragat 1, I-44122 Ferrara, Italy
burigana@iasfbo.inaf.it

ALESSANDRO GRUPPUSO

INAF–IASF Bologna, Via Piero Gobetti 101, I-40129 Bologna, Italy
INFN, Sezione di Bologna, Via Irnerio 46, I-40126, Bologna, Italy
gruppuso@iasfbo.inaf.it

PAOLO NATOLI

Dipartimento di Fisica e Scienze della Terra, Università degli Studi di Ferrara, Via Giuseppe Saragat 1, I-44122 Ferrara, Italy
INAF–IASF Bologna, Via Piero Gobetti 101, I-40129 Bologna, Italy
paolo.natoli@gmail.com

We provide a description of the latest status and performance of the *Planck* satellite, focusing on the final predicted sensitivity of *Planck*. The optimization of the observational strategy for the additional surveys following the nominal fifteen months of integration (about two surveys) originally allocated and the limitation represented by astrophysical foreground emissions are presented. An outline of early and intermediate astrophysical results from the *Planck* Collaboration is provided. A concise view of some fundamental cosmological results that will be achieved by exploiting *Planck's* full set of temperature and polarization data is presented. Finally, the perspectives opened by *Planck* in answering some key questions in fundamental physics, with particular attention to Parity symmetry analyses, are described.

Keywords: cosmology, cosmic background radiation, fundamental constants, neutrinos in astronomical observations, galaxy clusters, active galaxies, primordial galaxies, Milky Way, Zodiacal Light.

1. Introduction

The cosmic microwave background (CMB) is the most direct probe of the conditions of the very early Universe. Its study probes fundamental and particle physics at energy scales that are impossible to test using earthly laboratories. CMB and microwave emissions from astrophysical objects produce crucial information on cosmic

[*]Agenzia Spaziale Italiana, Viale Liegi 26, Roma, Italy

structure evolution at different sizes and distances. For this reason, great efforts have been dedicated to measure their properties with increasing accuracy. The *Planck* satellite[a,b] represents the third generation of space missions designed to map the microwave sky. The presentation of *Planck* observations[c] started in 2011, with the publication of the so-called *Planck* Early Papers (PEPs)[d]. The tremendous efforts in data analysis required to extract the cosmological information based on CMB maps necessitated a staggering of the data released; the release of the first products and results for 2013 will be followed by subsequent releases in the few next years.

In this review, we provide a description of the final sensitivity predicted for *Planck* and of the optimization of the observational strategy for its additional surveys following the nominal fifteen months of integration (about two surveys) originally allocated, discussing the limitation represented by astrophysical foreground emissions (Sect. 2). We then briefly summarize the main astrophysical results obtained with the early and intermediate paper releases (see [1] for a more complete review on these aspects), with a certain attention to two Galactic science topics recently achieved (Sect. 3). In Section 4 we give a concise view of some fundamental cosmological results that will be achieved with *Planck*, exploiting its full set of both temperature and polarization data. Finally, Section 5 is devoted to the perspectives opened by *Planck* in answering to some key questions in fundamental physics, giving particular attention to those topics investigated with Parity analyses.

2. The *Planck* mission

The *Planck* CMB anisotropy probe was launched into space on 14 May 2009 at 13:12:02 UTC, by an Ariane 5 ECA launcher, from the Guiana Space Centre, Kourou, French Guiana. As of mid July 2012, *Planck* was still successfully operating. *Planck* orbits around the L2 Lagrangian point and scans the sky spinning at 1 rpm in almost great circles with its Gregorian dual-reflector telescope pointing at 85° from the spin axis[2,3]. In the telescope focal plane the microwave photons are collected by two wide-band receiver arrays[4–7] spanning a frequency interval ranging from ∼30 GHz to ∼857 GHz, the Low Frequency Instrument (LFI) and the High Frequency Instrument (HFI). LFI is a coherent differential array based on 20 K InP HEMT[e] amplifiers covering the 30-70 GHz range in three bands centered at approximately 30, 44 and 70 GHz[8]. HFI is an array of bolometers cooled to 0.1 K

[a] *Planck* is a project of the European Space Agency - ESA - with instruments provided by two scientific Consortia funded by ESA member states (in particular the lead countries: France and Italy) with contributions from NASA (USA), and telescope reflectors provided in a collaboration between ESA and a scientific Consortium led and funded by Denmark.
[b] http://www.esa.int/Planck
[c] This paper is based largely on the *Planck* Early Release Compact Source Catalogue and publicly available publications by ESA and the *Planck* Collaboration, for what concerns the related aspects. Any material presented here that is not already described in *Planck* Collaboration papers represents the views of the authors and not necessarily those of the *Planck* Collaboration.
[d] http://www.sciops.esa.int/index.php?project=PLANCK&page=Planck_Published_Papers
[e] Indium Phosphide High Electron Mobility Transistor.

in nine frequency bands centered at 100, 143, 217, 353, 545 and 857 GHz [9]. LFI and HFI accumulated data together up to the consumption of the cryogenic liquids on January 2012, achieving $\simeq 29.5$ months of integration, corresponding to about five complete sky surveys. At this point, HFI was no longer able to operate. However, observations using the LFI are projected to continue. Moreover, *Planck* is sensitive to linear polarization up to 353 GHz. A summary of *Planck's* performance is provided in Table 1.

Table 1. *Planck* performances. The average sensitivity, δT/T, per FWHM^2 resolution element (FWHM is reported in arcmin) is given in CMB temperature units (i.e. equivalent thermodynamic temperature). The white noise (per frequency channel for LFI and per detector for HFI) in 1 sec of integration (NET, in μK $\cdot\sqrt{\text{s}}$) is also given in CMB temperature units. The other used acronyms are: DT = detector technology, N of R (or B) = number of radiometers (or bolometers), EB = effective bandwidth (in GHz). Note that at 100 GHz all bolometers are polarized, thus the temperature measure is derived combining data from polarized bolometers. Of course, the real sensitivity of the whole mission will have to include also the potential residuals of systematic effects. The *Planck* mission has been designed to suppress potential systematic effects down to $\simeq \mu$K level or below.

HFI	$\simeq 29.5$ months	of integration	($\simeq 5$ surveys)	
Frequency (GHz)	100	143	217	353
FWHM in T (P)	9.6 (9.6)	7.1 (6.9)	4.6 (4.6)	4.7 (4.6)
N of B in T (P)	(8)	4 (8)	4 (8)	4 (8)
EB in T (P)	33 (33)	43 (46)	72 (63)	99 (102)
NET in T (P)	100 (100)	62 (82)	91 (132)	277 (404)
δT/T [μK/K] in T (P)	2.04 (3.31)	1.56 (2.83)	3.31 (6.24)	13.7 (26.2)

HFI		
Frequency (GHz)	545	857
FWHM in T	4.7	4.3
N of B in T	4	4
EB in T	169	257
NET in T	2000	91000
δT/T [μK/K] in T	103	4134

LFI	$\simeq 29.5 + 21$ months	of integration	($\simeq 8$ surveys)
Frequency (GHz)	30	44	70
InP DT	MIC	MIC	MMIC
FWHM	33.34	26.81	13.03
N of R (or feeds)	4 (2)	6 (3)	12 (6)
EB	6	8.8	14
NET	159	197	158
δT/T [μK/K] (in T)	1.85	2.85	4.69
δT/T [μK/K] (in P)	2.61	4.02	6.64

2.1. *Planck extensions and scanning strategy optimization*

The spacecraft spin axis follows a cycloidal path across the sky in step-wise displacements of 2 arcmin. Since the projected position of the spin axis onto the ecliptic plane must advance steadily in longitude, the time interval between two maneuvers varies between 2360 s and 3904 s. The duration of the maneuvers themselves (averaging five minutes) varies between 6% and 12%, depending on the phase of the

cycloid. As *Planck* spins, the instrument beams cover near circles in the sky. The set of observations made during a period of fixed spin axis pointing is often referred to as a ring. As the Earth and *Planck* orbit the Sun, the observed circles rotate about the ecliptic poles. The amplitude of the spin-axis cycloid is chosen so that all the beams of both instruments cover the entire sky in one year. *Planck* tilts to cover first one Ecliptic pole, then tilts the other way to cover the other pole six months later. During the next six months, the satellite changes the direction of rotation on a given circle. The *Planck* beams scan the entire sky exactly twice in one year, but scan only about 95% of the sky in six months. For convenience, we call an approximately six month period a survey. Null tests between 1-year periods with the same cycloid phase are extremely powerful, while null tests between surveys are useful for many types of tests, but with some limitations.

Routine operations started on 12 August 2009. The fourth survey was shortened in order to start earlier with a slightly different scanning strategy (adopted for Surveys 5-8). The coverage of the fifth survey is smaller than that of the others due to gaps in the coverage from time spent in deep rings. During routine scanning, the *Planck* instruments naturally observe objects of special interest in order to calibrate receivers. These include Mars, Jupiter, Saturn, Uranus and Neptune, as well as the Crab Nebula. At the end of the fourth survey, the phase of the cycloid was shifted by 90 degrees, modifying the scanning directions throughout the sky in such a way that the combination of surveys before and after the change improved the range of polarizer angles on the sky, therefore helping in the treatment of systematic effects and improving polarization calibration. This change in scanning strategy applies to Surveys 5-8. The so-called nominal mission ended on 28 November 2010 and includes 15.5 months of data acquired during Surveys 1, 2, and part of 3. The HFI bolometers stopped producing useful scientific data on 13 January 2012 when the onboard supply of 3He needed to cool them to 0.1 K ran out. However, LFI continues to operate and acquire scientific data from the sky. The end of *Planck* operations is expected in the autumn of 2013. The satellites rotation speed was increased from 1 rpm to 1.4 rpm between 8 and 16 December 2011. During this period the planet Mars was observed. This operation was implemented to measure systematic effects on the scientific data linked to the spin rate. The total time lost due to anomalies is about 5 days spread over the 15.5 months of the nominal mission.

The main objective of the LFI-only extension of the *Planck* mission was to improve our knowledge of LFI systematic effects and calibration in order to optimize *Planck's* scientific yield. In particular, we identified four key instrument-related effects: (i) optical beam measurements through Jupiter mapping; (ii) polarization calibration and mapping of the Crab Nebula; (iii) effect of the shape of the bandpasses on polarization; and (iv) gain stability and noise properties. Recent developments in the *Planck* data analysis have introduced an additional key point, i.e., the need to optimize low multipole power spectra analysis. However, further analysis has shown that deep rings do not definitely provide an improvement, and an increased understanding of systematics is the principle reason for smooth scanning during most of

the LFI-only extension period. This allows us to accumulate additional surveys, and thus better characterize diffuse foregrounds at large angular scales and continue to measure all sources, providing a significant impact for long term variability studies.

The primary reasons for and effects of the optimal scanning strategy during the LFI-only extension can be summarized as follows:
1. Optical beam measurements – Detailed knowledge of the instruments beams and of the telescope optical parameters are key elements for the interpretation of *Planck* data, as they should be accounted for in many data analysis steps. Deep observations of Jupiter are very useful for improving the mapping of *Planck* LFI beams. During the first half of January 2012 HFI continued to observe Jupiter in order to study detector sidelobes and bolometer time constants.
2. polarization calibration – The Crab Nebula has been intensively observed in order to reduce the uncertainty in polarization orientation of the feed horns.
3. Bandpass effect on polarization – Bandpass mismatch is the main systematic effect for LFI polarization, also at low multipoles; this in turn has an impact on the polarization analysis of *Planck* as a whole. We performed detailed simulations to quantify the residual error in the leakage a-factors (which control the residual effect in the data) focusing on the LFI-only phase. Continuing with the smooth scan strategy, except for the two above-named calibration sources, was crucial to achieve the desired error reduction up to a factor of 3 for the 44 GHz channels. The primary cause of the improved recovery is the method of scanning the LMC over a large set of scanning angles.
4. Gain stability and noise properties – The determination of an accurate gain model is essential for LFI data analysis. The radiometer gain and noise properties are independent of the details of the scanning strategy, but smooth scanning allow jackknife tests to be performed with previous surveys, highlighting gain variation effects, particularly those due to thermal conditions of the FM1 cooler close to its end-of-life.
5. Jackknife tests – Smooth scanning is much more effective than deep annuli if an extra full-sky scan can be completed. New full-sky maps, using the phase shifted scheme, will allow for a number of powerful differential checks, particularly jackknife tests, which have already proved highly valuable in highlighting residual systematic effects, particularly at low multipoles.
6. Deep annuli for ancillary science – Deep annuli have been recognized useful for two ancillary science programs, Galactic and extragalactic foreground separation, and studies of extragalactic radio sources. The deep annuli greatly increase the LFI sensitivity in restricted regions and hence at small angular scales; the annuli planned for Jupiter and Crab Nebula observations have been designed for these purposes.

2.2. *Astrophysical foreground limitation*

CMB maps are contaminated by a significant level of foreground emission of both Galactic and extragalactic origin. As for polarization, the most critical Galactic

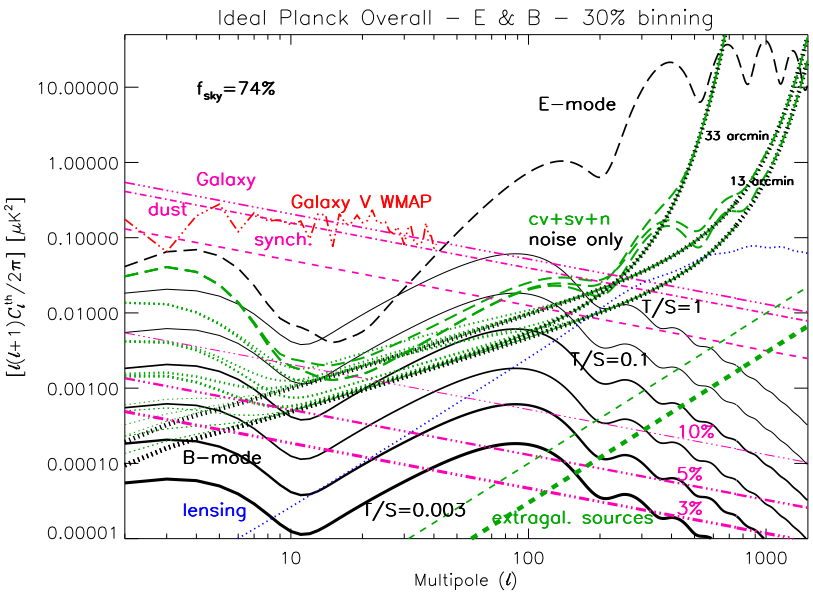

Fig. 1. CMB E polarization modes (black long dashes) compatible with *WMAP* data and CMB B polarization modes (black solid lines) for different tensor-to-scalar ratios $T/S = r$ of primordial perturbations are compared to *Planck*'s overall sensitivity to the power spectrum over two surveys as well as the whole mission. We assume that the expected noise had been subtracted, and that all frequency maps are smoothed to two different FWHM angular resolutions. The plots include cosmic and sampling variance plus instrumental noise based on Table 1 (green dots for B modes; green long dashes for E modes, labeled with cv+sv+n; black thick dots for noise only) assuming a multipole binning of 30%. Note that the cosmic and sampling (74% sky coverage excluding the sky regions mostly affected by Galactic emission) variance implies a dependence of the overall sensitivity on r at low multipoles, relevant to the parameter estimation; instrumental noise only determines the capability of detecting the B mode. The B mode induced by lensing (blue dots) is also shown for comparison. Galactic synchrotron (purple dashes) and dust (purple dot-dashes) polarized emissions produce the overall Galactic foreground (purple three dot-dashes). *WMAP* 3-yr power-law fits for uncorrelated dust and synchrotron emission have been used. For comparison, *WMAP* 3-yr results (http://lambda.gsfc.nasa.gov/) derived from the foreground maps using HEALPix tools[10] (http://healpix.jpl.nasa.gov/), are shown: power-law fits provide (generous) upper limits to the power at low multipoles. Residual contamination levels by Galactic foregrounds (purple three dot-dashes) are shown for 10%, 5%, and 3% of the map level, at increasing thickness. We also plot realistic estimates of the residual contribution of un-subtracted extragalactic sources, $C_\ell^{\rm res,PS}$ and the corresponding uncertainty, $\delta C_\ell^{\rm res,PS}$, respectively as thin and thick green dashes.

diffuse foregrounds are certainly synchrotron and thermal dust emissions, whereas the contribution of free-free emission is negligible. Other components, like spinning dust and haze, are still poorly known in polarization, while *Planck* temperature data recently allowed us to improve their comprehension. Synchrotron emission is the dominant Galactic foreground signal at low frequencies, up to ~ 60 GHz, where dust emission starts to dominate. At the *Planck* frequency channel of 70 GHz, Galactic foregrounds are at their minimum level, at least at angular scales above $\sim$ one

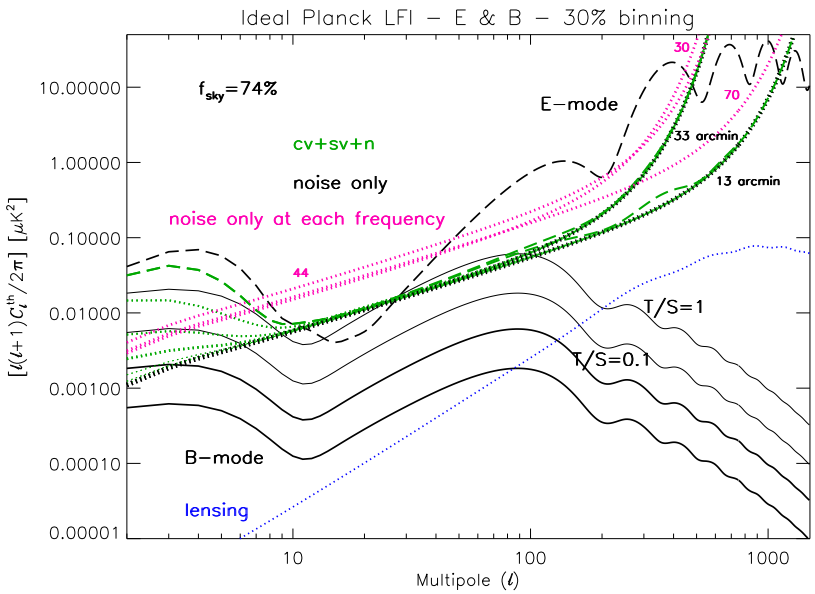

Fig. 2. The same as in Fig. 1 but for considering the overall sensitivity of LFI only and a smaller range of r. We report also the LFI sensitivity (noise only, red dots) at each frequency channel assuming the corresponding resolution (while, for simplicity, foregrounds are not included here).

degree. External galaxies are critical only at high ℓ, and extragalactic radio sources are likely the most crucial contributors to polarized signal up to frequencies ~ 200 GHz, which are the most suitable for CMB anisotropy experiments. Undetected extragalactic point sources contaminate the CMB angular power spectrum (APS) depending on their detection threshold, typically around $\simeq 0.1$ Jy. Except at very high multipoles, their residual effect is likely significantly below that coming from Galactic foregrounds.

In Fig. 1 we compare in terms of APS the overall sensitivity of *Planck* to polarization with potential contamination by foregrounds. Fig. 2 reports for comparison the overall sensitivity in polarization of *Planck* LFI as well as that achieved by each LFI frequency channel. In these figures, a realistic estimation of data losses from the rejection of data significantly affected by cosmic rays is also taken into account (while the decrease in sensitivity coming from neglecting the fraction of data during satellite spin axis repointing, about five minutes per hour, is not included, since, in principle, one can include also these data in refined analyses).

3. Astrophysical results

The first publications of *Planck's* main cosmological implications (i.e. based on CMB maps derived from *Planck*) are expected in early 2013, together with the delivery of a first set of *Planck* maps and cosmological products based on the first 15 months of data. They will be mainly based on temperature data.

Prior to the delivery of *Planck* products and cosmological results[f] (see [12] for descriptions of the *Planck* scientific programme), a first multifrequency view of the *Planck* astrophysical sky was presented on January 2011. The first scientific results, the PEPs, have been published by Astronomy and Astrophysics (EDP sciences) in the dedicated Volume 536 (December 2011). They describe the instrument performance in flight, including thermal behavior (PEPs I–IV), the LFI and HFI data analysis pipelines (PEPs V–VI), the main astrophysical results regarding Galactic science (PEPs XIX–XXV), extragalactic sources and far-IR background (PEPs XIII–XVIII), and Sunyaev-Zel'dovich effects and cluster properties (PEPs VIII–XII and XXVI). These papers have been complemented by a subsequent work on blazars based on a combination of high energy and *Planck* observations[13] . The first *Planck* sky maps form the basis of the construction of the *Planck* Early Release Compact Source Catalog (ERCSC) (see PEP VII and *The Explanatory Supplement to the Planck Early Release Compact Source Catalogue*), which was the first *Planck* product delivered to the scientific community. Of course, by accumulating sky surveys and refining data analysis, the *Planck* sensitivity to point sources will significantly improve in next years. The forthcoming *Planck* Legacy Catalog of Compact Sources (PCCS), to be released in early 2013 and to be updated in the subsequent years, will represent one of the major *Planck* products relevant for multi-frequency studies of compact or point–like sources.

A further set of astrophysical results has been presented at the conference *Astrophysics from radio to sub-millimeter wavelengths: the Planck view and other experiments* held in Bologna on 13-17 February 2012[g]. Several articles, constituting the set of so-called *Planck* Intermediate Papers (PIPs), have already been submitted in 2012 (PIPs I-X, at the date of October 2012; see again footnote d) and others are in preparation. *Planck* papers will be roughly divided into two categories: those based only on total intensity data, and those requiring well established (and, typically, with a longer time schedule) polarization data. Among the various topics addressed by PIPs, the currently available papers mainly focus on cluster physics and their cosmological relevance; these papers, derived from *Plank* data, analyze the Sunyaev-Zel'dovich effect (in combination with X-ray data from XMM-Newton and the microwave ground-based interferometer AMI) and the improvement achieved on number counts and spectral indices of extragalactic, infrared and radio sources (see [14] for a review on these topics).

[f]This Meeting took place well before the *Planck* cosmological release, occurred later in March 2013. The reader interested in the nominal (i.e. two surveys) temperature *Planck* analyses can refer to the papers available at project web site and to [11] for a summary. We focus here on some results available at the time of this Meeting and to selected cosmological and fundamental physics perspectives achievable with the full mission.

[g]http://www.iasfbo.inaf.it/events/planck-2012/

3.1. *Two remarkable Galactic science results*

By using precise full-sky observations from *Planck*, and applying several methods of component separation, the emission from the Galactic haze at microwave wavelengths has been identified and characterized[15]. The haze is a distinct component of diffuse Galactic emission, roughly centered on the Galactic centre, and extends to $|b| \sim 35^\circ - 50^\circ$ in Galactic latitude and $|l| \sim 15^\circ - 20^\circ$ in longitude. By combining WMAP and *Planck* data, [15] were able to determine the spectrum of this emission to high accuracy, unhindered by the large systematic biases present in previous analyses. The derived spectrum is consistent with power-law emission with a spectral index of -2.56 ± 0.05, thus ruling out free-free emission as the source and instead favouring hard-spectrum synchrotron radiation. The underlying electron population should have a spectrum (number density per energy) $dN/dE \sim E^{-2.1}$.

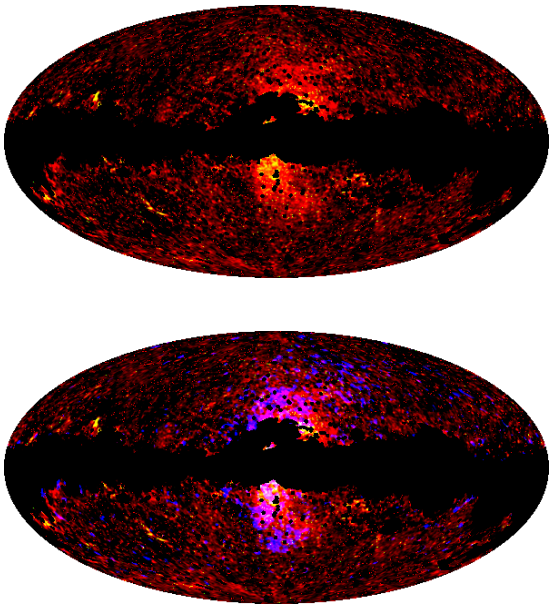

Fig. 3. *Top*: The microwave haze at *Planck* 30 GHz (red, -12 μK $< \Delta T_{\rm CMB} <$ 30 μK) and 44 GHz (yellow, 12 μK $< \Delta T_{\rm CMB} <$ 40 μK). *Bottom*: The same but including the *Fermi* 2-5 GeV haze/bubbles[16] (blue, 1.05 $<$ intensity [keV cm^{-2} s^{-1} sr^{-1}] $<$ 1.25; see their Fig. 11).

As shown in Fig. 3 (from [15]), at Galactic latitudes $|b| < 30^\circ$ the microwave haze spatial morphology is consistent with that of the Fermi gamma-ray "haze" or "bubbles", particularly at low southern Galactic latitude, suggesting that the same underlying physical mechanism is observed in two very different frequency domains (see also [17]). It is unlikely to explain the very hard spectrum and the extended nature of the emission in terms of supernova shocks in the Galactic disk. A new

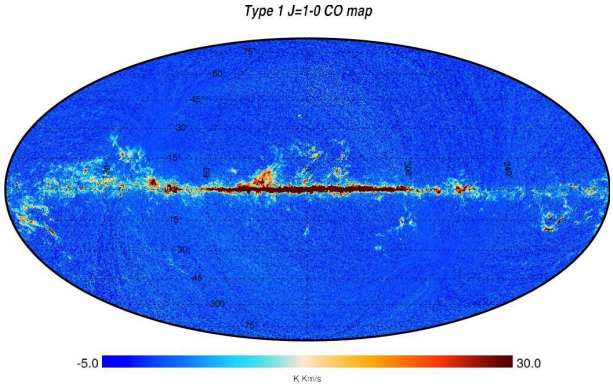

Fig. 4. Full-sky CO $J = 1 \rightarrow 0$ (at 115.271 GHz) map Galactic coordinates derived in the single-channel approach (type 1) exploiting differences in the spectral transmission of the line among the bolometers (pairs of bolometers) of the HFI 100 GHz channel. Different methods give consistent results. Extraction methods based on the use of more channels improves the signal to noise ratio of the map. The map is smoothed to 15 arcmin and has a pixel resolution of 1.7 arcmin corresponding to $N_{side} = 2048$ in HEALPix scheme. Similar maps are obtained for the other transition lines.

mechanism for cosmic-ray acceleration in the Galactic centre is needed.

Lastly, we recall the extraction of the CO maps from *Planck* data performed with two different component separation methods. Rotational transition lines of CO play a major role in molecular radio astronomy and in particular in the study of star formation and the Galactic structure. A wealth of data exists in the Galactic plane and some well-known molecular clouds, but no CO high sensitivity all-sky survey was available. In general, molecular line emission could contribute to the signal in some frequency bands, that are typically relatively wide in order to increase the measurement sensitivities. CO all-sky surveys have been constructed using the *Planck* HFI data because the three lowest CO rotational transition lines at 115, 230 and 345 GHz significantly contribute to the signal of the 100, 217 and 353 GHz HFI channels respectively[7] .

The *Planck* map of CO Galactic emission[18] (see Fig. 4, adapted from [18]) can be used to search for faint CO emission associated with the dark-gas and to guide ground-based follow-up observations.

4. Cosmological perspectives

Due to its high sensitivity and resolution covering the whole sky and to its wide frequency coverage allowing a substantial progress in foreground modeling and removal, *Planck* will open a new era in our understanding of the Universe and its astrophysical structures.

Some of the analyses will be carried out through a precise measurement of the temperature, polarization and correlations of CMB APS, whereas others, in particular those related to the geometry of the Universe and to the research of non-Gaussianity signatures, will be based on the exploitation of the anisotropy pattern.

The most ambitious goal is the possible detection of the so-called B-mode APS.

Planck will improve the accuracy of current measurements over a wide set of cosmological parameters by a factor of ~ 3 to ~ 10 and will characterize the geometry of the Universe with unprecedented accuracy. *Planck* will elucidate our understanding of a wide range of unresolved cosmological issues, ranging from the early stages of the Universe, to the evolution of cosmic structures, to the characterization of primordial conditions and perturbations, to the late phases of cosmological reionization.

4.1. *Cosmological reionization*

The beginning of the reionization process is approximately identified by the Thomson optical depth, τ. Under various hypotheses (the simple ΛCDM model, the inclusion of curvature and dark energy, different kinds of isocurvature modes, of neutrino properties, of primordial He mass fraction, of tensor perturbation, of running, etc.) the best fit values of τ compatible with WMAP data, possibly complemented with external data, typically lie in the range $\sim 0.08-0.1$, with the exact interval depending on the considered cosmological model and combination of data sets. The 68% CL uncertainty on τ is of $\simeq \pm 0.013 - 0.015$, nearly independent of the considered case.

While this simple "τ-parametrization" of the reionization process and, in particular, of its imprints on the CMB anisotropy likely represents a sufficiently accurate modeling for the interpretation of current CMB data, great attention has been recently focused on the accurate computation of the reionization signatures in the CMB for a large variety of astrophysical scenarios and physical processes (see e.g. [19-27]) with a view towards incorporating results of forthcoming and future experiments (see [28] for a review). Note that current *Planck* cosmological results, based on temperature data, rely on WMAP for polarization constraints (crucial for reionization).

In [29] a detailed study of the impact of reionization on galaxy formaions (and the associated radiative feedback) and of the corresponding detectable signatures has been presented. The study's particular focus is a detailed comparison of two well defined alternative prescriptions (*suppression* and *filtering*) for the radiative feedback mechanism suppressing star formation in small-mass halos; thus, the study shows that they are consistent with a wide set of existing observational data but predict different 21 cm background signals accessible to future observations (see also [30] for a different astrophysical reionization model). The corresponding signatures detectable in the CMB have been computed in [31]. Different scenarios have been investigated in [32] assuming that structure formation and/or extra sources of energy injection in the cosmic plasma can induce a double reionization epoch of the Universe at low (*late* processes) or high (*early* processes) redshifts, providing suitable analytical representations, called hereafter as "phenomenological reionization histories". In the late models, hydrogen was typically thought to be first ionized at

higher redshifts ($z \sim 15$, mimicking a possible effect by Pop III stars) and then at lower redshifts ($z \sim 6$, mimicking the effect by stars in galaxies), while in the early reionization framework the authors hypothesized a *peak-like reionization* induced by energy injection in the cosmic plasma at $z \gtrsim$ some $\times\, 10^2$.

The sensitivity improvement of CMB polarization experiments calls for a complete and accurate characterization of all CMB APS, including the polarization B-modes, from low to high multipoles. Especially useful studies include those by [33] and [34] for the connection of B-modes with inflation and their detectability, by [35] for the analysis of the kinetic Sunyaev-Zel'dovich effect from mildly non-linear large-scale structure, and by [36] on the computation of B-modes induced by lensing. In [37] the wide sets of astrophysical and phenomenological models quoted above are analyzed through detailed computations of the signatures they produce in the CMB temperature and polarization anisotropies, discussing the impact of next *Planck* data release and the interplay with primordial B-mode analyses.

5. Fundamental physics

The *Planck* perspectives on important selected topics linking cosmology to fundamental physics (for instance, neutrino masses and effective species number, the primordial helium abundance, various fundamental constants of physics, the parity property of CMB maps and its connection with CPT symmetry with an emphasis on the Cosmic Birefringence, the detection of the stochastic field of gravitational waves) will also show how *Planck* represents an extremely powerful *fundamental and particle physics laboratory.*

5.1. *Constraints on neutrino properties and on the variation of fundamental constants*

The sum of neutrino masses (three in the standard scenario) $\sum m_\nu$ has an impact on CMB power spectra. Current observational constraints are in the sub-eV scale, so neutrinos are (still) relativistic at recombination and effect on the anisotropy spectra is small. At large and moderate angular scales the integrated Sachs-Wolfe (ISW) changes the spectrum roughly around the first acoustic peak. Not surprisingly, the ISW effect is the main probe for neutrino masses before *Planck*. The high resolution of *Planck* will allow measurements in a region of the anisotropy spectrum (at high multipole ℓ) where gravitational lensing provides a new window on neutrino masses. Hence, *Planck* is expected to significantly tighten the constraints, attaining $\sum m_\nu \lesssim 0.7$eV for temperature only measurement and about half of that from temperature and polarization [38]. Combination with dataset that also probe the matter distribution (e.g., baryon acoustic oscillations or BAO) should also significantly tighten the constraints.

Another neutrino related parameter that*Planck* should constrain well is the effective neutrino number, $N_{\rm eff}$, which parametrizes the density of radiation in the Universe (not counting the CMB). This parameter specifies the energy density when

the species are relativistic, by means of a neutrino effective temperature when assuming three flavours. In the Standard Model, $N_{\rm eff} = 3.046$, where the small deviation from 3 is due to the fact that the cosmological parameter is defined assuming instantaneous decoupling. There is a weak evidence today for $N_{\rm eff} > 3$, which could open up the case for a neutrino/antineutrino asymmetry, or an even more intriguing extra (sterile) neutrino. Hence, the *Planck* measurements are long awaited. In the case of temperature and polarization, *Planck* alone should be able to attain a $\sigma_{N_{\rm eff}} \simeq 0.2$ at 68% CL, a value that could be further reduced by 50% or better using other datasets [38].

Finally, an interesting probe of fundamental physics can be obtained by constraint the variation of fundamental constants, most interesting the fine structure constant α. The latter can be constrained by the CMB because a variation would impact light to matter interactions and, hence, the anisotropy spectrum. At observationally useful sensitivities, the effect is small, but competitive bounds could be set by CMB observations, probing a range of redshift space different from those traditionally employed in astronomical bounds on the variations of α (e.g., through quasars). *Planck* is expected to yield $\sim 0.2\%$ accuracy on α variations, which could possibly be reduced below 0.1% by using complementary cosmological datasets (e.g, high resolution CMB polarization experiments such as the predicted ACTPol [38]).

5.1.1. *Hydrogen $2S \to 1S$ transition rate*

The two photon decay of $2S$-level determines the rate of recombination of hydrogen in the "middle recombination layer", where the pattern of CMB polarization is formed. Therefore, precise cosmological data could allow us to estimate A_{2s1s}-constant with rather high accuracy. Currently, the decay rate A_{2s1s} is theoretically calculated[39,40] to be $8.22458\,{\rm s}^{-1}$. However, there is very little experimental verification of this because the corresponding experiments are difficult[41] . Experimentally, 2S-1S two photon transition has been measured in [42-44] for the decay of K-shell vacancy in an initially neutral atom using the photon-photon coincidence technique. In these experiments, the K-shell vacancy is produced by irradiating the targets using photons or radioactive isotopes, preferably ones decaying by nuclear electron capture. However, all these experiments mainly are devoted to the investigation of heavy ions, rather then hydrogen atoms.

Since the rate of cosmic recombination during its most important stage is mainly determined by the two-photon decay rate A_{2s1s}, the CMB anisotropy correlation functions are rather sensitive to the value of A_{2s1s}. By using `RECFAST` and `CAMB` code (see [45-48]) with small modifications, [49] have computed CMB power spectra for various values of A_{2s1s} and compared theoretical predictions with WMAP CMB data in combination with the Hubble Constant measurement, the Hubble Space Telescope (HST), Baryonic Acoustic Oscillation (BAO) data from SDSS and WiggleZ, and Big Bang Nucleosynthesis constraint[50–53] , in order to reduce the uncertainty on the Hubble parameter. Analyzing the Markov chains produced by the

CosmoMC[54], [49] obtained the following constraint: $6.24\mathrm{s}^{-1} < A_{2s1s} < 11.89\mathrm{s}^{-1}$ and $4.47\mathrm{s}^{-1} < A_{2s1s} < 14.67\mathrm{s}^{-1}$ with 1 and 2 σ confidence, respectively.

The upcoming *Planck* data are expected to provide a very tight constraint on A_{2s1s}, thanks to the low noise polarization data and the temperature data of high angular resolution. *Planck* mock data was generated up to the multipole $\ell = 2000$ by the publicly available FUTURCMB code[55] with the sensitivity expected from the first two surveys[12]. The TT, TE, EE power spectrum was analyzed with CosmoMC assuming the WMAP concordance model, the decay rate A_{2s1s} to $8.22458\,\mathrm{s}^{-1}$, and exploiting three high sensitivity channels with a sky fraction 0.65: [49] found $8.086\mathrm{s}^{-1} < A_{2s1s} < 9.037\mathrm{s}^{-1}$ and $7.613\mathrm{s}^{-1} < A_{2s1s} < 9.505\mathrm{s}^{-1}$ at 1σ and 2σ level, respectively, i.e. an estimated error on A_{2s1s} of $\simeq 0.486\,\mathrm{s}^{-1}$, which is less than 6 % of the central value. An improvement of this prediction is obviously expected once the whole set of *Planck* surveys can be exploited.

5.2. *Fundamental physics from CMB Parity analyses*

The statistical properties of the CMB pattern may be used to constrain Parity (P) symmetry.

Linear polarization maps are components of a rank two tensor[56] and are decomposed by the spin harmonics $a_{\pm 2,\ell m} = \int d\Omega\, Y^{\star}_{\pm 2,\ell m}(\hat{n})\,(Q(\hat{n}) \pm iU(\hat{n}))$, where $Y_{\pm 2,\ell m}(\hat{n})$ are Spherical Harmonics of spin 2 and $a_{\pm 2,\ell m}$ are the corresponding coefficients. It is then useful to introduce new coefficients as linear combinations of the previous: $a_{E,\ell m} = -(a_{2,\ell m} + a_{-2,\ell m})/2$ and $a_{B,\ell m} = -(a_{2,\ell m} - a_{-2,\ell m})/2i$. These have opposite behaviors under a P transformation: $a_{E,\ell m} \rightarrow (-1)^{\ell}\, a_{E,\ell m}$, $a_{B,\ell m} \rightarrow (-1)^{\ell+1}\, a_{B,\ell m}$. If P is conserved, by combining the previous transformation one immediately derives that the cross-correlations $C_{\ell}^{TB} = \langle a^{\star}_{T,\ell m} a_{B,\ell' m'} \rangle$ and $C_{\ell}^{EB} = \langle a^{\star}_{E,\ell m} a_{B,\ell' m'} \rangle$ must vanish. Further details can be found in [56,57] and explicit algebra is set forth in the Appendix of [58]. Parity violation, however, may change this scenario.

Parity violations arise in two models: as modification of electromagnetism[59–61] or as modification of the standard picture of the Inflationary mechanism, where P is broken due to primordial (chiral) gravitational waves[62–64]. Both of these scenarios predict non null cross-correlations between gradient and curl modes and between scalar and curl modes in the CMB polarization pattern. However, chiral gravity produces such correlations at the CMB last scattering surface (impacting the lowest modes of these cross-correlations), whereas general modification of the standard electromagnetism produces cross-correlations other than zero even at higher multipoles. To perform these kinds of analyses, it has become customary not to use the aforementioned cross-correlations but a related estimator called the cosmological birefringence angle, which is defined as the rotation angle of polarization plane during the CMB photon journey from its last scattering to us[65]. The impact of such a rotation on the CMB angular power spectra (in the limit of constant α) is given

by[62,66–68]:

$$\langle C_\ell^{TE,obs}\rangle = \langle C_\ell^{TE}\rangle \cos(2\alpha)\,, \tag{1}$$
$$\langle C_\ell^{TB,obs}\rangle = \langle C_\ell^{TE}\rangle \sin(2\alpha)\,, \tag{2}$$
$$\langle C_\ell^{EE,obs}\rangle = \langle C_\ell^{EE}\rangle \cos^2(2\alpha) + \langle C_\ell^{BB}\rangle \sin^2(2\alpha)\,, \tag{3}$$
$$\langle C_\ell^{BB,obs}\rangle = \langle C_\ell^{BB}\rangle \cos^2(2\alpha) + \langle C_\ell^{EE}\rangle \sin^2(2\alpha)\,, \tag{4}$$
$$\langle C_\ell^{EB,obs}\rangle = \frac{1}{2}\left(\langle C_\ell^{EE}\rangle + \langle C_\ell^{BB}\rangle\right)\sin(4\alpha)\,, \tag{5}$$

where the label ^{obs} stands for observed. We mainly report here the findings from [69].

5.2.1. *Cosmological birefringence*

The WMAP team[70] reported $\alpha^{\mathrm{WMAP\,7yr}} = -0.9^\circ \pm 1.4^\circ$ at 68% C.L.. Our constraint, obtained at low resolution[69] (the same estimator as has been used in [71]), reads $\alpha = -1.6^\circ \pm 1.7^\circ$ (3.4°) at 68% (95%) C.L. for $\Delta\ell = 2-47$ (see red curve of the right panel of Fig. 5; from [69]). Considering $\Delta\ell = 2-23$ we obtain $\alpha = -3.0^{\circ\,+2.6^\circ}_{\,-2.5^\circ}$ at 68% C.L. and $\alpha = -3.0^{\circ\,+6.9^\circ}_{\,-4.7^\circ}$ at 95% C.L. (see red curve of middle panel of Fig. 5). This is the same multipole range considered by the WMAP team at low resolution

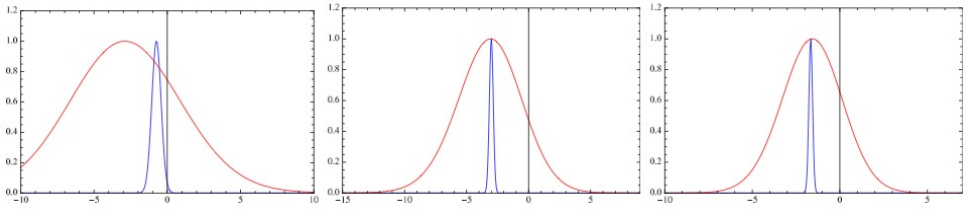

Fig. 5. Joint likelihood of α for $\Delta\ell = 2-6$ in the left panel, $\Delta\ell = 2-23$ in the middle panel and $\Delta\ell = 2-47$ in the right panel. Red designates the WMAP data and blue the *Planck* forecast. See also the text.

in [70] (the only other result available in the literature at these large angular scales). With a pixel based likelihood analysis they obtained $\alpha^{\mathrm{WMAP\,7yr}} = -3.8^\circ \pm 5.2^\circ$ at 68% C.L.. For a smaller multipole range, i.e. $\Delta\ell = 2-6$, see red curve of left panel of Fig. 5.

When specializing suitable multipole ranges, using the estimator defined in [71], it is possible to extract the spectrum of α, i.e. α vs ℓ, see Fig. 6 (from [69]), in search of a possible scale dependence of the birefringence effect. The results are compatible with no detection at all angular scales probed here.

In [72], where a birefringence analysis is performed at high multipoles, it is claimed that the improvement expected for the *Planck* satellite[2] in terms of sensitivity[12] is of a factor around 15. Almost the same number is obtained here (see blue curves in all the panels of Fig. 5) for the *Planck* likelihoods computed from

hypothetical *Planck* observations of WMAP data at *Planck*'s own noise amplitude. Both forecasts only consider the nominal sensitivity, whereas uncertainties due to systematic effects are not taken into account.

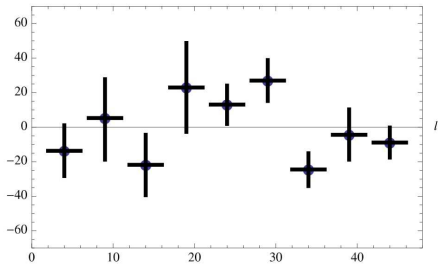

Fig. 6. The dot represents the peak position and the error bars provides the 1σ C.L.. See also the text.

To date, the constraints obtained on the angle of birefringence from WMAP[73], QUAD[74], BICEP[75] and Boomerang[76] are compatible with zero, while WMAP is not sensitive enough to detect circular gravitational waves[65,69]. This research field (among others) closely anticipates scientific results that will be achieved with *Planck* polarization data.

Acknowledgements – We thank the Editorial Board of Astronomy and Astrophysics (European Southern Observatory; ESO) for having granted us the permission to reproduce two figures originally published in (or submitted to) the same Journal. It is a pleasure to thank the Editorial Board of Journal of Cosmology and Astroparticle Physics (Institute of Physics, IOP, Publishing) for the opportunity to reproduce two figures originally published in the same Journal. Credits are indicated when each figure is mentioned in the text for the first time. We warmly thank the *Planck* Collaboration and, in particular, all the members of the *Planck* HFI and LFI Core Teams, with whom they shared the analysis and the interpretation of *Planck* data, as well as the subjects discussed here. We also warmly thank the members of the *Planck* Science Team and Editorial Board for the permission of publishing this paper. A particular thank to Benjamin Walter for the careful reading of the paper that helped us in text improvement. We acknowledge support by ASI through ASI/INAF Agreement I/072/09/0 for the Planck LFI Activity of Phase E2. CB, AG, and PN acknowledge also partial support by MIUR through PRIN 2009 grant n. 2009XZ54H2.

References

1. C. Burigana *et al.*, *IJMPD* **22/6** (2013) 1330011.
2. *Planck* Collab. I, *Astron. Astrophys.* **536** (2011) A1.
3. J. A. Tauber *et al.*, *Astron. Astrophys.* **520** (2010) A2.
4. A. Mennella *et al.*, *Astron. Astrophys.* **536** (2011) A3.

5. *Planck* HFI Core Team (P. A. R. Ade *et al.*), *Astron. Astrophys.* **536** (2011) A4.
6. A. Zacchei *et al.*, *Astron. Astrophys.* **536** (2011) A5.
7. *Planck* HFI Core Team (P. A. R. Ade *et al.*), *Astron. Astrophys.* **536** (2011) A6.
8. M. Bersanelli *et al.*, *Astron. Astrophys.* **520** (2010) A4.
9. J.-M. Lamarre *et al.*, *Astron. Astrophys.* **520** (2010) A9.
10. K.M. Gorski, E. Hivon, A.J. Banday, B.D. Wandelt, F.K. Hansen, M. Reinecke and M. Bartelmann, *Astrophys. J.* **622** (2005) 759.
11. *Planck* Collaboration, *Planck* 2013 results. I. *Astron. Astrophys.* submitted (2013) arXiv://1303.5062.
12. *Planck* Collab. The Scientific Programme of Planck, ESA publication ESA-SCI (2005)/1, arXiv://0604069.
13. P. Giommi *et al.*, *Astron. Astrophys.* **541** (2012) A160.
14. L. Toffolatti, C. Burigana, F. Argüeso and J.M. Diego, *Extragalactic Compact Sources in the Planck Sky and their Cosmological Implications* in: Open Book "Open Questions in Cosmology", Edited by Gonzalo Olmo (IFIC - Spain) and published by InTechOpen (2012) Chapter 3, p. 57-86, arXiv://1302.3355.
15. *Planck* Collab. IX *Astron. Astrophys.* **554** (2013) A139.
16. G. Dobler, D. P. Finkbeiner, I. Cholis, T. Slatyer, and N. Weiner, *The Astrophys. J.* **717** (2010) 825.
17. E. Carretti *et al.*, *Nature* **493** (2012) 66.
18. *Planck* Collab. *Planck* 2013 results. XIII, submitted to *Astron. Astrophys.* (2013), arXiv://1303.5073v2.
19. P.J.E. Peebles, S. Seager, W. Hu, *The Astrophys. J.* **539** (2000) L1.
20. A.G. Doroshkevich and P.D. Naselsky, *Phys. Rev. D* **65** (2002) 13517.
21. R. Cen, *The Astrophys. J.* **591** (2003) 12.
22. B. Ciardi, A. Ferrara and S.M.D. White, *Mon. Not. R. Astron. Soc.* **344** (2003) L7.
23. A.G. Doroshkevich, I.P. Naselsky, P.D. Naselsky and I.D. Novikov, *The Astrophys. J.* **586** (2002) 709.
24. S. Kasuya, M. Kawasaki and N. Sugiyama, *Phys. Rev. D* **69** (2004) 023512.
25. S.H. Hansen and Z. Haiman, *The Astrophys. J.* **600** (2004) 26.
26. L.A. Popa, C. Burigana and N. Mandolesi, *New Astronomy* **11** (2005) 173.
27. J.S.B. Wyithe and R. Cen, *The Astrophys. J.* **659** (2007) 890.
28. C. Burigana, F. Finelli, R. Salvaterra, L.A. Popa and N. Mandolesi, *Recent Res. Devel. Astronomy & Astrophys.* **2** (2004) 59.
29. R. Schneider, R. Salvaterra, T.R. Choudhury, A. Ferrara, C. Burigana and L.A. Popa, *Mon. Not. R. Astron. Soc.* **384** (2008) 1525.
30. R. Salvaterra, A. Ferrara and P. Dayal, *Mon. Not. R. Astron. Soc.* **414** (2011) 847.
31. C. Burigana, L.A. Popa, R. Salvaterra, R. Schneider, T.R. Choudhury and A. Ferrara, *Mon. Not. R. Astron. Soc.* **404** (2008) 385.
32. P. Naselsky and L.Y. Chiang, *Mon. Not. R. Astron. Soc.* **347** (2004) 795N.
33. U. Seljak and M. Zaldarriaga, Phys. Rev. Lett. **78** (1997) 2054.
34. M. Kamionkowski and A. Kosowsky, *Phys. Rev. D* **57** (1998) 685.
35. W. Hu, *The Astrophys. J.* **529** (2000) 12.
36. U. Seljak and C.M. Hirata, *Phys. Rev. D* **69** (2004) 043005.
37. T. Trombetti and C. Burigana, *J. Modern Physics* **3** (2012)1918.
38. S. Galli *et al*, *Phys. Rev. D* **82** (2010) 123504.
39. S. P. Goldman, *Phys. Rev. A* **40** (1989).
40. L. Spitzer, Jr. and J. L. Greenstein, *The Astrophys. J.* **114** (1951) 407.
41. D. O'Connell, K. J. Kollath, A. J. Duncan, and H. Kleinpoppen, *Journal of Physics B Atomic Molecular Physics* **8** (1975) L214.

42. Y. B. Bannett and I. Freund, *Two-photon inner-shell transitions in molybdenum*, *Phys. Rev. A* **30** (1984) 299.
43. X.-M. Tong, J.-M. Li, L. Kissel, and R. H. Pratt, *Phys. Rev. A* **42** (1990) 1442.
44. R. W. Dunford, E. P. Kanter, B. Krässig, S. H. Southworth, L. Young, P. H. Mokler, and T. Stöhlker, *Phys. Rev. A* **67** (2003) 0545501.
45. S. Seager, D. Sasselov, and D. Scott, *The Astrophys. J.* **523** (1999) L1.
46. S. Seager, D. Sasselov, and D. Scott, *The Astrophys. J.* **128** (2000) 407.
47. W. Y. Wong, A. Moss, and D. Scott, *Mon. Not. R. Astron. Soc.* **386** (2008) 1023.
48. A. Lewis, A. Challinor, and A. Lasenby, *The Astrophys. J.* **538** (2000) 473. http://camb.info/.
49. V. Mukhanov, J. Kim, P. Naselsky, T. Trombetti and C. Burigana, *J. Cosmol. Astropart. Phys.* **6** (2012) 40.
50. A. G. Riess, L. Macri, S. Casertano, M. Sosey, H. Lampeitl, H. C. Ferguson, A. V. Filippenko, S. W. Jha, W. Li, R. Chornock, and D. Sarkar, *The Astrophys. J.* **699** (2009) 539.
51. C. Blake, E. A. Kazin, F. Beutler, T. M. Davis, D. Parkinson, S. Brough, M. Colless, C. Contreras, W. Couch, S. Croom, D. Croton, M. J. Drinkwater, K. Forster, D. Gilbank, M. Gladders, K. Glazebrook, B. Jelliffe, R. J. Jurek, I.-H. Li, B. Madore, D. C. Martin, K. Pimbblet, G. B. Poole, M. Pracy, R. Sharp, E. Wisnioski, D. Woods, T. K. Wyder, and H. K. C. Yee, *Mon. Not. R. Astron. Soc.* **418** (2011) 1707.
52. W. J. Percival, B. A. Reid, D. J. Eisenstein, N. A. Bahcall, T. Budavari, J. A. Frieman, M. Fukugita, J. E. Gunn, Ž. Ivezić, G. R. Knapp, R. G. Kron, J. Loveday, R. H. Lupton, T. A. McKay, A. Meiksin, R. C. Nichol, A. C. Pope, D. J. Schlegel, D. P. Schneider, D. N. Spergel, C. Stoughton, M. A. Strauss, A. S. Szalay, M. Tegmark, M. S. Vogeley, D. H. Weinberg, D. G. York, and I. Zehavi, *Mon. Not. R. Astron. Soc.* **401** (2010) 2148.
53. G. Steigman, *International Journal of Modern Physics E* **15** (2006) 1.
54. A. Lewis and S. Bridle, *Phys. Rev. D* **66** (2002) 103511.
55. L. Perotto, J. Lesgourgues, S. Hannestad, H. Tu, and Y. Y Y Wong, *J. Cosmol. Astropart. Phys.* **10** (2006) 013.
56. M. Zaldarriaga and U. Seljak, *Phys. Rev. D* **55**, 1830 (1997).
57. M. Zaldarriaga, *The Astrophys. J.* **503** (1998) 1.
58. A. Gruppuso, F. Finelli, P. Natoli, F. Paci, P. Cabella, A. De Rosa and N. Mandolesi, *Mon. Not. R. Astron. Soc.* **411** (2011) 1445.
59. S. M. Carroll, G. B. Field and R. Jackiw, *Phys. Rev. D* **41** (1990) 1231.
60. S. M. Carroll and G. B. Field, *Phys. Rev. D* **43** (1991) 3789.
61. S. M. Carroll, *Phys. Rev. Lett.*, **81** (1998) 3067.
62. A. Lue, L. -M. Wang and M. Kamionkowski, *Phys. Rev. Lett.* **83** (1999) 1506.
63. S. Saito, K. Ichiki and A. Taruya, *J. Cosmol. Astropart. Phys.* **0709** (2006) 002.
64. L. Sorbo, *J. Cosmol. Astropart. Phys.* **1106** (2011) 003.
65. V. Gluscevic and M. Kamionkowski, *Phys. Rev. D* **81** (2010) 123529.
66. B. Feng, M. Li, J.-Q. Xia, X. Chen, X. Zhang, *Phys. Rev. Lett.* **96** (2006) 221302.
67. B. Feng, H. Li, M. Li and X. Zhang, *Phys. Lett.* **B620** (2005) 27.
68. WMAP Collab. (E. Komatsu *et al.*), *Astrophys. J. Suppl.* **180** (2009) 330.
69. A. Gruppuso, P. Natoli, N. Mandolesi, A. De Rosa, F. Finelli and F. Paci, *J. Cosmol. Astropart. Phys.* **1202** (2012) 023.
70. WMAP Collab. (E. Komatsu *et al.*), *Astrophys. J. Suppl.* **192** (2011) 18.
71. QUaD Collab. (E. Y. S. Wu *et al.*), *Phys. Rev. Lett.* **102** (2009) 161302.
72. G. Gubitosi, L. Pagano, G. Amelino-Camelia, A. Melchiorri and A. Cooray, *J. Cosmol. Astropart. Phys.* **8** (2009) 21.

73. WMAP Collab. (G. Hinshaw *et al.*), accepted to *Astrophys. J. Suppl.* (2013), arXiv:1212.5226v3 [astro-ph.CO].
74. QUaD Collab. (M. L. Brown *et al.*), *The Astrophys. J.* **705** (2009) 978.
75. J. -Q. Xia, H. Li and X. Zhang, *Phys. Lett. B* **687** (2010) 129.
76. L. Pagano *et al.*, *Phys. Rev. D* **80** (2009) 043522.